Journal of Power Sources 189 (2009) 752–756

Contents lists available at ScienceDirect

Journal of Power Sources

journal homepage: www.elsevier.com/locate/jpowsour

Short communication

Effects of Co doping on $Li[Ni_{0.5}Co_xMn_{1.5-x}]O_4$ spinel materials for 5 V lithium secondary batteries via Co-precipitation

Sung Woo Oh [a], Seung-Taek Myung [b,**], Han Byeol Kang [a], Yang-Kook Sun [a,*]

[a] Department of Chemical Engineering, Hanyang University, Seoul 133-791, South Korea
[b] Department of Chemical Engineering, Iwate University, 4-3-5 Ueda, Morioka, Iwate 020-8551, Japan

ARTICLE INFO

Article history:
Received 27 June 2008
Received in revised form 5 August 2008
Accepted 6 August 2008
Available online 20 August 2008

Keywords:
$Li[Ni_{0.5}Mn_{1.5}]O_4$
5 V
Positive
Electrode
Lithium
Batteries

ABSTRACT

Effect of Co substitution for Mn on $Li[Ni_{0.5}Co_xMn_{1.5-x}]O_4$ was investigated. Co-precipitation was employed to synthesize the $[Ni_{0.25}Co_xMn_{0.75-x}](OH)_2$ as a precursor and it was fired with LiOH at 900 °C for 20 h in air. From Rietveld refinement of X-ray diffraction data and scanning electron microscopic examinations, it was found that the as-synthesized $Li[Ni_{0.5}Co_xMn_{1.5-x}]O_4$ were crystallized in cubic spinel structure with *Fd*3*m* space group and the final products presented spherical secondary morphology (3 μm in average). Electrochemical investigation revealed that Co^{3+} replacement for Mn^{4+} gave rise to improved rate and cycling performances probably due to the improved electronic conductivity and structural stability achieved by the presence of Co^{3+} in the spinel $Li[Ni_{0.5}Co_xMn_{1.5-x}]O_4$.

1. Introduction

Manganese spinel and its derivatives have been studied extensively because of their cost advantages and environmentally friendliness as cathode materials for Li-ion batteries [1]. Transitional metal substituted spinel especially with the composition of $Li[M_{0.5}Mn_{1.5}]O_4$ (M = Cr, Co, Fe, Ni, Mg, Cu, etc.) shows a higher voltage plateau at around 5 V [2–7]. Among them, $LiNi_{0.5}Mn_{1.5}O_4$ with a flat high voltage profile has received a great deal of attention because of high voltage profile [8–15]. It has been considered that above 4.5 V the electrolyte currently used in Li-ion batteries usually starts to decompose which means the stable electrochemical voltage window has been limited below 4.5 V.

However, the increasing demands on high power properties of Li-ion battery for hybrid electric vehicle and plug-in hybrid electric vehicle applications lead the research efforts to explore the high voltage cathode materials. Although side reactions due to the instability of electrolyte at high voltage (>4.5 V) on the electrode surface can substantially deteriorate the cycling behavior of the $Li[Ni_{0.5}Mn_{1.5}]O_4$, the better understanding and research effort is necessary to improve the electrochemical performances of high voltage $Li[Ni_{0.5}Mn_{1.5}]O_4$ material.

In this study, we investigated structural and electrochemical properties of Co-doped $Li[Ni_{0.5}Co_xMn_{1.5-x}]O_4$ ($x = 0$ and 0.05) spinel material with various doping amount of Co.

2. Experimental

Spherical precursor $[Ni_{0.25}Co_xMn_{0.75-x}](OH)_2$ ($x = 0$ and 0.025) compounds were synthesized by co-precipitation method [16]. The appropriate amounts of $NiSO_4{\cdot}6H_2O$, $CoSO_4{\cdot}6H_2O$ and $MnSO_4{\cdot}5H_2O$ were used as the starting materials for the synthesis of $[Ni_{0.5}Co_xMn_{1.5-x}](OH)_2$ ($x = 0$ and 0.05). An aqueous solution of $NiSO_4{\cdot}6H_2O$, $CoSO_4{\cdot}6H_2O$ and $MnSO_4{\cdot}5H_2O$ with a concentration of 2.4 mol L^{-1} was pumped into a continuously stirred tank reactor (CSTR, 4L) under a N_2 atmosphere. At the same time, NaOH solution (aq.) of 4.8 mol L^{-1} and desired amount of NH_4OH solution (aq.) as a chelating agent were also separately pumped into the reactor. The concentration of the solution, pH, temperature, and stirring speed of the mixture in the reactor were carefully controlled. After control these conditions, the microscale hydroxides (3 μm) were obtained. Then, the $[Ni_{0.25}Co_xMn_{0.75-x}](OH)_2$ ($x = 0$ and 0.025) powders were filtered and washed using distillated water. The obtained spherical particles dried at 110 °C to remove adsorbed water. The obtained $[Ni_{0.25}Co_xMn_{0.75-x}](OH)_2$ ($x = 0$ and 0.025) compounds were thoroughly mixed with appropriate amount of $LiOH{\cdot}H_2O$ (molar ratio

* Corresponding author. Tel.: +82 2 2220 0524; fax: +82 2 2282 7329.
** Corresponding author. Tel.: +81 19 621 6345; fax: +81 19 621 6345.
E-mail addresses: smyung@iwate-u.ac.jp (S.-T. Myung), yksun@hanyang.ac.kr (Y.-K. Sun).

0378-7753/$ – see front matter © 2008 Elsevier B.V. All rights reserved.
doi:10.1016/j.jpowsour.2008.08.022

of Li/transition metals = 1.05) and calcined at 900 °C for 20 h in air.

Powder X-ray diffraction (XRD, Rigaku, Rint-2200) using Cu Kα radiation was used to identify crystalline phase of the prepared powders. XRD data were obtained at $2\theta = 10$–$110°$, with a step size of 0.03°. The collected intensity data of XRD were analyzed by the Rietveld refinement program *Fullprof* 2002 [17]. The morphology of prepared powders was also observed using scanning electron microscopy (SEM, JSM-6340F, JEOL). Chemical compositions were analyzed with an atomic absorption spectroscopy (Vario 6, Analyticjena). BET surface area measurements were done by the nitrogen adsorption–desorption method (Autosorb-1, QUANTACHROME Instruments).

The positive electrode was prepared by blending the $Li[Ni_{0.5}Co_xMn_{1.5-x}]O_4$ ($x = 0$ and 0.05) active materials, Super P carbon black, and polyvinylidene fluoride (85:7.5:7.5) in *N*-methyl-2-pyrrolidone. The slurry was cast on aluminum foil and dried at 110 °C for 10 h in a vacuum oven. Disks were punched out of the foil. Lithium foil was used as a negative electrode. The electrochemical characterizations were carried out using 2032 coin type cell with 1 M $LiPF_6$ solution in ethylene carbonate (EC)–diethyl carbonate (DEC) mixture (1:1 in volume, Cheil Industries). Positive electrode and lithium metal negative electrode were separated by the porous polypropylene film. Charge–discharge tests were performed with a current density of 70 mA g^{-1} (0.5 *C*-rate) at 30 °C. AC-impedance measurements were performed using a Zahner Elektrik IM6 impedance analyzer over the frequency range from 1 MHz to 1 mHz with an amplitude of 10 mV_{rms}.

3. Results and discussion

Fig. 1 shows Rietveld refinement results of XRD data for $Li[Ni_{0.5}Co_xMn_{1.5-x}]O_4$ ($x = 0$ and 0.05). The prepared materials present a well-crystallized cubic spinel structure with *Fd*3*m* space group. To confirm the occupation of Co element as a dopant, Rietveld refinements were done by assuming that 8*b* and 16*c* sites are vacant. Occupation factors of all elements are invariable, based on the results of chemical analysis for the final products: $Li_{1.00}[Ni_{0.49}Mn_{0.51}]O_4$ and $Li_{1.00}[Ni_{0.45}Co_{0.05}Mn_{0.50}]O_4$. It is believed from the AAS results that the excess amount of lithium compensated for the lithium evaporation during high temperature calcination. The observed peaks were well matched with the calculated one in Fig. 1a and b with 10.9% and 11.1% of R_{wp} values, respectively, which represents high reliability. This implies that those elements are well located in their own sites. Lattice parameters obtained by the refinement were $a = 8.165(4)$ Å and $a = 8.168(3)$ Å, whose values are close to those reported [2,8–12]. In fact, the ionic radius of Mn^{4+} (0.53 Å, coordination: VI [18]) is slightly smaller than that of Co^{3+} (0.545 Å, low spin, coordination: VI [18]). This would affect the variation in the lattice parameter by Co substitution for Mn in $Li[Ni_{0.5}Co_xMn_{1.5-x}]O_4$. It further evidences the occupation of Co in the tetravalent Mn sites in the spinel compound. From the rietveld refinements, it is found that single-phase $Li[Ni_{0.5}Co_xMn_{1.5-x}]O_4$ ($x = 0$ and 0.05) were successfully formed via co-precipitation.

Fig. 2 shows SEM images of as-synthesized $Li[Ni_{0.5}Co_xMn_{1.5-x}]O_4$ ($x = 0$ and 0.05) powders. They have spherical morphology in secondary particles, and average particle size estimated was almost 3 μm in Fig. 2a and b. The primary particles for $Li[Ni_{0.5}Mn_{1.5}]O_4$ were needle-like shape in Fig. 2a and they were densely agglomerated in secondary forms. Co replacement resulted in morphological change in primary particles in Fig. 2b; the bar-like particles were partially changed to octahedron-like shape. Growth of primary particles were also observed by Co substitution for Mn in $Li[Ni_{0.5}Co_xMn_{1.5-x}]O_4$.

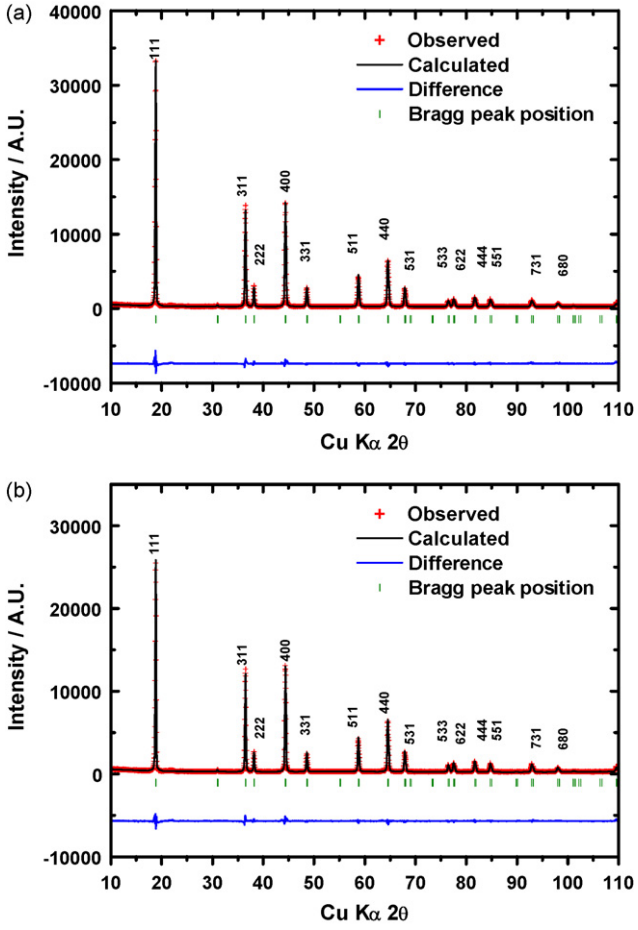

Fig. 1. Rietveld refinement results of XRD data for $Li[Ni_{0.5}Co_xMn_{1.5-x}]O_4$: (a) $x = 0$ and (b) $x = 0.05$.

The electrochemical properties of the $Li[Ni_{0.5}Co_xMn_{1.5-x}]O_4$ ($x = 0$ and 0.05) materials were investigated. The charge–discharge profiles between 3.5 and 5 V at 30 °C are shown in Fig. 3. The cells were charged and discharged by applying a constant current of 70 mA g^{-1} (0.5 *C*-rate). Both cells present two distinct plateaus at around 4.7 V that are attributed to the $Ni^{2+/3+/4+}$ redox couple [2,8–12]. A small plateau in the 4 V region was also observed that arise from the Mn^{3+} and Mn^{4+} redox couple in Fig. 3a. In ideal $Li[Ni_{0.5}Mn_{1.5}]O_4$ structure, the oxidation state of Mn is fixed at +4 [2,8–12]. As reported, however, an oxygen deficiency appears in $Li[Ni_{0.5}Mn_{1.5}]O_4$ when it prepared at higher temperature, and this partially lowers the oxidation state of Mn from 4+ to 3+ [8,9].

Co-free $Li[Ni_{0.5}Mn_{1.5}]O_4$ delivered a discharge of about 140 mAh g^{-1} in Fig. 3a. Meanwhile, Co replacement resulted in reduced discharge capacity, 130 mAh g^{-1}. Since the trivalent Co element is located in the tetravalent Mn sites, the obtained capacity is expected to be higher than that of $Li[Ni_{0.5}Mn_{1.5}]O_4$. As reported by Kawai et al. [19,20], when Co^{3+} appears in the spinel structure, it is electrochemically active above 5 V versus Li, accompanying by a $Co^{3+/4+}$ redox couple. This implies that the $Co^{3+/4+}$ redox in the spinel structure is scarcely observed in the 4 V region. That is why Co-doped $Li[Co_xMn_{2-x}]O_4$ spinels had a lower capacity with increasing Co content in 4 V region [21,22]. In consideration of thermodynamic data, the Gibbs energies ($\Delta_f G°$) of formation at 298 K for NiO, Co_3O_4, and MnO_2 are −211.7, −774, −465.2 kJ mol^{-1}, respectively [23]. From these data, we can imagine that the introduction of Co^{3+} can change the resulting ionicity

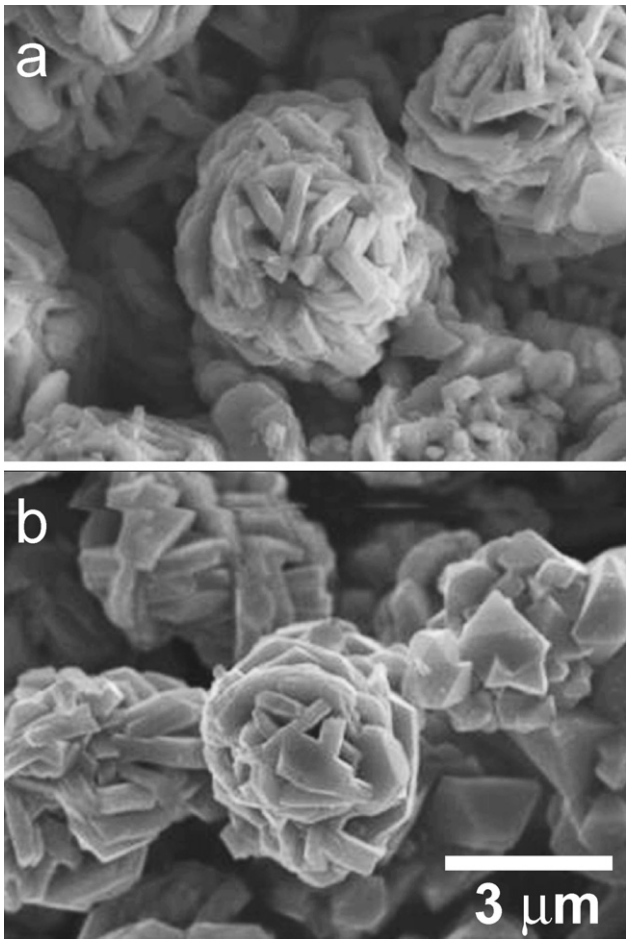

Fig. 2. SEM images of $Li[Ni_{0.5}Co_xMn_{1.5-x}]O_4$: (a) $x = 0$ and (b) $x = 0.05$.

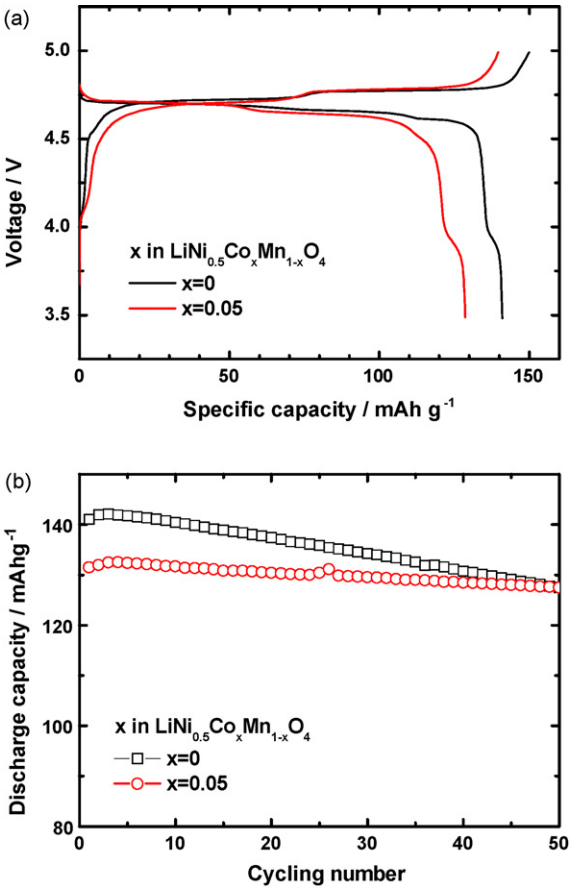

Fig. 3. (a) Initial charge and discharge curves of $Li[Ni_{0.5}Co_xMn_{1.5-x}]O_4$ ($x = 0$ and 0.05) and (b) corresponding cyclability. A constant current density of 70 mA g^{-1} was applied across the positive electrodes at 30 °C.

and covalency in the structure. That is, bonding strength of transition metal element and oxygen can be strengthened by the incorporation of trivalent Co in the structure. Thus, if the cell is operated at a much lower current and if the cell is charged to much higher voltage cutoff, i.e., 5.5 V, $Li[Ni_{0.5}Co_{0.05}Mn_{1.45}]O_4$ would have much higher discharge capacity with help of $Ni^{2+/3+/4+}$ and $Co^{3+/4+}$ redox.

Although the capacity of $Li[Ni_{0.5}Co_{0.05}Mn_{1.45}]O_4$ is slightly smaller compared with the Co-free $Li[Ni_{0.5}Mn_{1.5}]O_4$, the reinforced structure by Co substitution for Mn site in $Li[Ni_{0.5}Co_{0.05}Mn_{1.45}]O_4$ would be responsible for the significantly improved cyclability in Fig. 3b. The capacity retention was of about 97% upon cycling for the $Li[Ni_{0.5}Co_{0.05}Mn_{1.45}]O_4$, while the retention for the Co-free $Li[Ni_{0.5}Mn_{1.5}]O_4$ was around 90% of its initial capacity.

The discharge curves of $Li/Li[Ni_{0.5}Co_xMn_{1.5-x}]O_4$ ($x = 0$ and 0.05) cells between 3.0 and 5.0 V at various current densities from 70 mA g^{-1} (0.5 *C*-rate) to 1400 mA g^{-1} (10 *C*-rates) are shown in Fig. 4. The cell was charged using a current density of 0.5 *C*-rate before each discharge test. With increasing currents, the Co-free $Li[Ni_{0.5}Mn_{1.5}]O_4$ exhibited a gradual decrease in capacity with lower operation voltage in Fig. 4a. A greater resistance is also seen with currents. At 5 *C*-rates (700 mA g^{-1}), the obtained capacity was only around 100 mAh g^{-1}. Furthermore, the capacity was less than 10 mAh g^{-1} at 10 *C*-rates (1400 mA g^{-1}) in Fig. 4a. In contrast, Co-doped $Li[Ni_{0.5}Co_xMn_{1.5-x}]O_4$ demonstrated relatively higher discharge voltage even at higher currents in Fig. 4b. For example, the average operation voltage was around 4.4 V versus Li at 5 *C*-rates (700 mA g^{-1}) with a higher discharge of 118 mAh g^{-1}. Even at 10 *C*-rates (1400 mA g^{-1}), it delivered a discharge capacity of 103 mAh g^{-1} in Fig. 4b. The average operation voltage was around 4 V versus Li at the current for the Co-doped $Li[Ni_{0.5}Co_{0.05}Mn_{1.45}]O_4$. It is most likely that the contained Co^{3+} in the oxide matrix improves electronic conductivity of $Li[Ni_{0.5}Mn_{1.5}]O_4$.

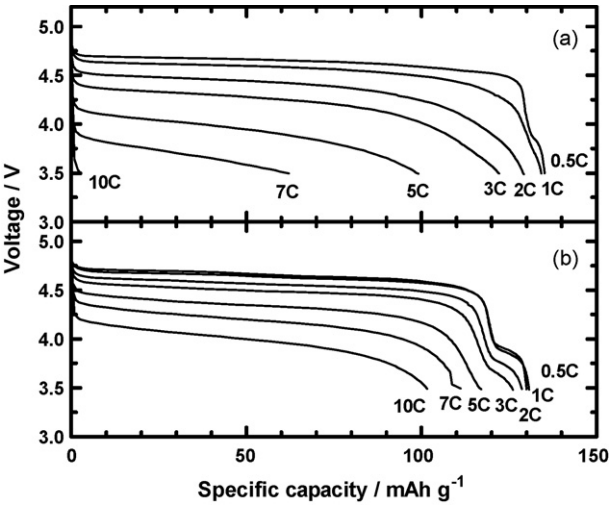

Fig. 4. Rate capabilities of $Li[Ni_{0.5}Co_xMn_{1.5-x}]O_4$: (a) $x = 0$ and (b) $x = 0.05$.

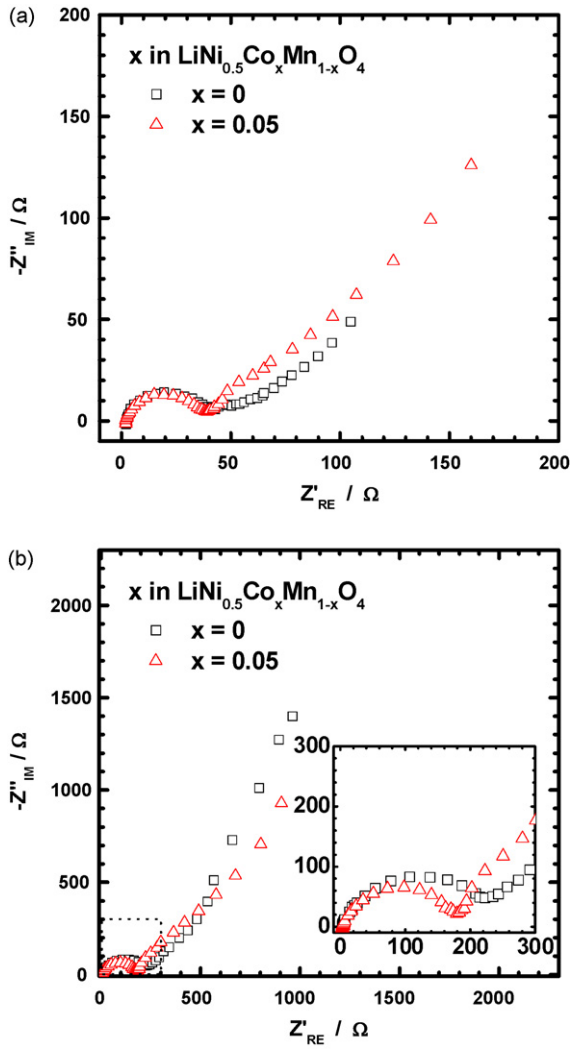

Fig. 5. Cole–Cole plots of $Li[Ni_{0.5}Co_xMn_{1.5-x}]O_4$ ($x = 0$ and 0.05): (a) before charging and (b) after 50 cycles.

To investigate the possible reason of improved cycling performance of the Co-doped $Li[Ni_{0.5}Co_{0.05}Mn_{1.45}]O_4$ electrochemical impedance spectroscopy (EIS) for the $Li[Ni_{0.5}Mn_{1.5}]O_4$ and the Co-doped $Li[Ni_{0.5}Co_{0.05}Mn_{1.45}]O_4$ were measured before and after cycling at 70 mA g^{-1} (0.5 *C*-rate) at 30 °C in Fig. 5. Before cycling the resistances for both electrodes seem to be close each other in the high to medium frequency range in Fig. 5a. After cycling, the resulting resistances for both electrodes obviously increased. In inset of Fig. 5b, it is clear that the Co-doped $Li[Ni_{0.5}Co_{0.05}Mn_{1.45}]O_4$ gave rise to the smaller charge transfer resistance relative to $Li[Ni_{0.5}Mn_{1.4}]O_4$ electrode. As described in Table 1, the dissolved amount of transition metal elements for the charged electrodes appeared smaller for the Co-doped $Li[Ni_{0.5}Co_{0.05}Mn_{1.45}]O_4$, since it is believed that the Co^{3+} incorporation into the structure would provide much stronger bond in the lattice. It, consequently, would affect the smaller charge transfer resistance in Fig. 5. Therefore, it is concluded that the introduction of $Co3^+$ to Mn^{4+} sites of $Li[Ni_{0.5}Mn_{1.5}]O_4$ is substantially effective to improve rate and cycling performances of $Li[Ni_{0.5}Mn_{1.5}]O_4$.

Table 1
Dissolved amounts of transition metal elements, Ni, Co, and Mn after charging to 5 V

Fully charged electrodes	Dissolved amount of transition metals		
	Ni/ppm	Mn/ppm	Co/ppm
$LiNi_{0.5}Mn_{1.5}O_4$	9.51	18.56	–
$LiNi_{0.5}Co_{0.05}Mn_{1.45}O_4$	4.39	12.85	4.7

The delithiated electrodes were stored at 60 °C for 300 h in the electrolyte.

4. Conclusions

In attempt to understand the effect of Co on $Li[Ni_{0.5}Co_xMn_{1.5-x}]O_4$, structural and electrochemical properties of $Li[Ni_{0.5}Co_xMn_{1.5-x}]O_4$ synthesized via co-precipitation were investigated. The as-synthesized $Li[Ni_{0.5}Co_xMn_{1.5-x}]O_4$ presented a spherical secondary morphology with 3 μm of diameter. Rietveld refinements of XRD data showed that the formed products had a cubic spinel structure with space group of *Fd*3*m* and revealed that the introduced Co^{3+} was well located in the Mn^{4+} sites in $Li[Ni_{0.5}Co_xMn_{1.5-x}]O_4$. Due to the similarity of ionic radii between Co^{3+} and Mn^{4+}, the resulting lattice parameters slightly differed from each other. On the other hand, the Co-doped $Li[Ni_{0.5}Co_xMn_{1.5-x}]O_4$ had significantly improved cycling stability and rate capability as well, probably due to the enhanced electronic conductivity and structural stability due to the stronger bonding character of Co–O in the structure. Therefore, substitution of Co^{3+} for Mn^{4+} was effective to improve the battery performances. Further work is now in progress to reveal the reaction mechanism and the origin of improved electrochemical performance of the Co-doped $Li[Ni_{0.5}Co_{0.05}Mn_{1.45}]O_4$.

Acknowledgement

This work was supported by the University IT Research Center Project.

References

[1] K. Amine, H. Tukamoto, H. Yasuda, Y.A. Fujita, J. Electrochem. Soc. 143 (1996) 1607.
[2] M. Yoshio, T. Konishi, Y.M. Todorov, H. Noguchi, Electrochemistry 68 (2000) 412.
[3] C. Sigala, A. Le Gal La Salle, Y. Piffard, D. Guyomard, J. Electrochem. Soc. 148 (2001) A812.
[4] H. Shigemura, H. Sakaebe, H. Kageyama, H. Kobayahsi, A.R. West, R. Kanno, S. Morimoto, S. Nasu, M. Tabuchi, J. Electrochem. Soc. 148 (2001) A730.
[5] Y. Ein-Eil, W.F. Howard, S.H. Lu, S. Mukerjee, J. McBreen, J.T. Vaughey, M.M. Thackeray, J. Electrochem. Soc. 145 (1998) 1238.
[6] Q. Zhong, A. Bonakdarpour, M. Zhang, Y. Gao, J.R. Dahn, J. Electrochem. Soc. 144 (1997) 205.
[7] P. Strobel, A. Ibarra Palos, M. Anne, F. Le Cras, J. Mater. Chem. 10 (2000) 429.
[8] S.-T. Myung, S. Komaba, N. Kumagai, H. Yashiro, H.-T. Chung, T.-H. Cho, Electrochim. Acta 47 (2002) 2543.
[9] J.-H. Kim, S.-T. Myung, C.S. Yoon, S.G. Kang, Y.-K. Sun, Chem. Mater. 16 (2004) 906.
[10] J.-H. Kim, S.-T. Myung, Y.-K. Sun, Electrochim. Acta 49 (2004) 219.
[11] J.-H. Kim, C.S. Yoon, S.-T. Myung, J. Prakash, Y.-K. Sun, Electrochem. Solid-State Lett. 7 (2004) A216.
[12] S.-H. Park, S.-W. Oh, S.-T. Myung, Y.-K. Sun, Electrochem. Solid-State Lett. 7 (2004) A451.
[13] D. Li, A. Ito, K. Kobayakawa, H. Noguchi, Y. Sato, J. Power Sources 161 (2006) 1241.
[14] K. Ariyoshi, Y. Iwakoshi, N. Nakayama, T. Ohzuku, J. Electrochem. Soc. 151 (2004) A296.
[15] Y. Idemoto, H. Sekine, K. Ui, N. Koura, Solid State Ionics 176 (2005) 299.
[16] M.-H. Lee, Y.-J. Kang, S.-T. Myung, Y.-K. Sun, Electrochim. Acta 50 (2004) 939.
[17] T. Roisnel, J. Rodriguez-Carjaval, Fullprof Manual, Institut Laue-Langevin, Grnoble, 2002.
[18] R.D. Shannon, Acta Crystallogr. Sect. A A32 (1976) 751.

[19] H. Kawai, M. Nagata, H. Tukamoto, A.R. West, Electrochem. Solid-State Lett. 1 (1998) 212.
[20] H. Kawai, M. Nagata, H. Kageyama, H. Tukamoto, A.R. West, Electrochim. Acta 45 (1999) 315.
[21] I. Taniguchi, D. Song, M. Wakihara, J. Power Sources 109 (2002) 333.
[22] Z. Wang, H. Ikuta, Y. Uchimoto, M. Wakihara, J. Electrochem. Soc. 150 (2003) A1250.
[23] J.A. Dean, Lange's Handbook of Chemistry, fourth ed., McGraw-Hill Inc., New York, 1992, p. 6.81.